

Damage Modelling of Automobile Components of Aluminium Materials under Crash Loading

Andrea Ockewitz, Dong-Zhi Sun

Fraunhofer-Institut für Werkstoffmechanik
Freiburg

Herbert Klamser, Daniel Malcher
Porsche AG, Weissach

Summary:

The crash behaviour of automobile components from an aluminium die cast alloy and from an extruded profile was characterised under different load conditions and simulated with two damage models (Gurson, Johnson-Cook). The influences of the stress triaxiality and strain rate on the deformation and damage behaviour were taken into account in the experimental and numerical investigation. The Gurson model was extended to simulate shear failure by using an additional failure criterion for the region between pure shear and uniaxial tension. To verify the damage models component tests under crash relevant loadings were performed and simulated with the damage parameters which were obtained by modelling the tension and shear tests on small scale specimens. The Gurson model and the Johnson-Cook model were compared with regard to the applicability of the damage parameters for different stress triaxialities. It was found that the Gurson model with the parameters from tension tests can be also applied to local loading situations with high stress triaxialities while the Johnson-Cook model requires additional fracture mechanics tests to determine the corresponding fracture strains for this kind of application.

Keywords:

Damage models, characterisation, extruded aluminium profiles, aluminium cast alloy, component tests, crash simulations

1 Introduction

Although crash simulations have been successfully used for the development and evaluation of new vehicles in automobile industry, there are still many requirements on the improvement of the quality of crash simulations. One of them is the modelling of damage behaviour of automobile components under crash loading. Crash simulations without taking into account damage behaviour can dramatically overestimate the load-carrying capacity and the absorbed energy of a structural component [1]. The application of new light weight materials e.g. magnesium, aluminium alloys and high strength steels makes damage modelling more important since these materials show a higher strength but lower ductility in comparison with conventional materials. Although different damage models [2-5] are available in crash codes, most crash simulations do not take into account the damage behaviour. The reason for the lack of damage modelling is that there are no systematic results concerning the questions which damage model gives a reliable prediction and how the damage parameters should be determined. Many phenomenological damage models need a lot of experiments which are usually not realised due to the costs.

The purpose of this work is the development and validation of the available damage concept used in [1] under complex loading and the determination of damage parameters for two automobile components. A component from an aluminium die cast alloy and from an extruded profile were characterised under crash relevant loading and simulated with two damage models. Tension and shear tests on specimens were performed to determine the damage parameters and component tests in different load cases were carried out to verify the damage models. By means of the two examples the micromechanical Gurson model was compared with the phenomenological Johnson-Cook damage model.

2 Damage modelling

The micro-mechanisms of ductile rupture are described by three phases i.e. void nucleation, growth and coalescence. The void growth depends not only on the equivalent plastic strain but also on triaxiality σ_m/σ_e which is defined as the ratio of the mean stress σ_m to the von Mises effective stress σ_e . Therefore, damage behaviour of a component depends strongly on load type e.g. tension, bending, compression or shear and on geometry e.g. thickness, notch radius. In addition, the damage behaviour is influenced by strain rate.

The damage models which are available in the commercial crash codes like LS-DYNA, Pam-Crash and ABAQUS/Explicit or as user subroutines for the commercial codes, can be divided into two groups: phenomenological models (e.g. Johnson-Cook, D_cR_c, FLD) and micromechanical models (e.g. Gurson and extended Gologanu). The phenomenological models are easy for application but they need a lot of experiments for the determination of their damage parameters. The micromechanical models which were derived on the basis of micro-mechanisms of material damage describe the influence of stress triaxiality on damage behaviour and therefore, their damage parameters are independent of specimen geometry. As examples a micromechanical model (Gurson) and a phenomenological model (Johnson-Cook) are briefly presented here.

2.1 Micromechanical damage model (Gurson)

The Gurson model modified by Needleman and Tvergaard [2] uses the yield condition

$$\Phi = \frac{\sigma_e^2}{\sigma_M^2} + 2q_1 f^* \cosh\left(\frac{tr\sigma}{2\sigma_M}\right) - 1 - (q_1 f^*)^2 = 0$$

Here, σ denotes the macroscopic stress tensor, σ_e the equivalent von Mises stress, σ_M the actual yield stress of the matrix material and f^* a function of void volume fraction f given by

$$f^*(f) = \begin{cases} f & \text{if } f < f_c \\ f_c + \frac{1/q_1 - f_c}{f_f - f_c} (f - f_c) & \text{if } f > f_c \end{cases}$$

where f_c and f_f are the critical void volume fractions at the onset of coalescence and at final rupture. The evolution equation for the porosity consists of the growth of existing voids and nucleation of new voids:

$$\dot{f} = (1-f)tr\dot{\epsilon}^{pl} + A\dot{\epsilon}_M^{pl} \quad , \quad A = \frac{f_n}{s_n\sqrt{2\pi}} e^{-1/2\left(\frac{\epsilon_M^{pl}-\epsilon_N}{s_N}\right)^2}$$

The variables $tr\dot{\epsilon}^{pl}$ and $\dot{\epsilon}_M^{pl}$ are the rate of the plastic volumetric strain and the rate of plastic equivalent strain of the matrix material. The advantage of the Gurson model is its micromechanical background and the physical meaning of the damage parameters e.g. porosity. In total, seven damage parameters (ϵ_N , s_N , q_1 , f_0 , f_n , f_c , f_f) have to be determined for the Gurson model. In section 3.2 a simple method for the determination of the Gurson parameters will be presented.

A limitation of the Gurson model for the application to crash simulations is that it does not describe shear failure. Two concepts have been developed to extend the Gurson model. The first one is the calculation of void shape in addition to void volume fraction using the Gologanu model [3] and the application of two different local failure criteria [6]. The second one is a combination of the Gurson model with a phenomenological criterion (Johnson-Cook) which is only used for the load region between pure shear and uniaxial tension. In this work the second concept was used.

2.2 Phenomenological damage model (Johnson-Cook)

The Johnson-Cook damage model [5] is based on a plastic fracture strain which depends on triaxiality (σ_m/σ_e), strain rate and temperature. Failure occurs when the damage variable D reaches the value 1. The equations below show the definition of the damage variable D and the plastic fracture strain ϵ_f . The symbol $\Delta\epsilon_e^p$ denotes the increment of the von Mises equivalent plastic strain. $\dot{\epsilon}_e^p$ and $\dot{\epsilon}_0$ are the rate of the von Mises equivalent plastic strain and of the reference strain. Since temperature was not changed in this work, the term describing the influence of temperature on damage is omitted. The material parameters d_1 , d_2 , d_3 and d_4 have to be determined by specimen tests under different triaxialities. In contrast to continuum damage models the Johnson-cook model uses the von Mises yield condition and the damage variable D does not affect the yield surface.

$$D = \sum \left(\frac{\Delta\epsilon_e^p}{\epsilon_f} \right) \geq 1 \quad , \quad \epsilon_f = d_1 + d_2 \exp(-d_3 \frac{\sigma_m}{\sigma_e}) \left[1 + d_4 \ln \left(\frac{\dot{\epsilon}_e^p}{\dot{\epsilon}_0} \right) \right]$$

3 Crash behaviour of a bumper from an extruded aluminium profile

The first automobile component investigated in this work was a bumper which consists of an extruded aluminium profile (7000 alloy). Its geometry is shown in Fig. 1b.

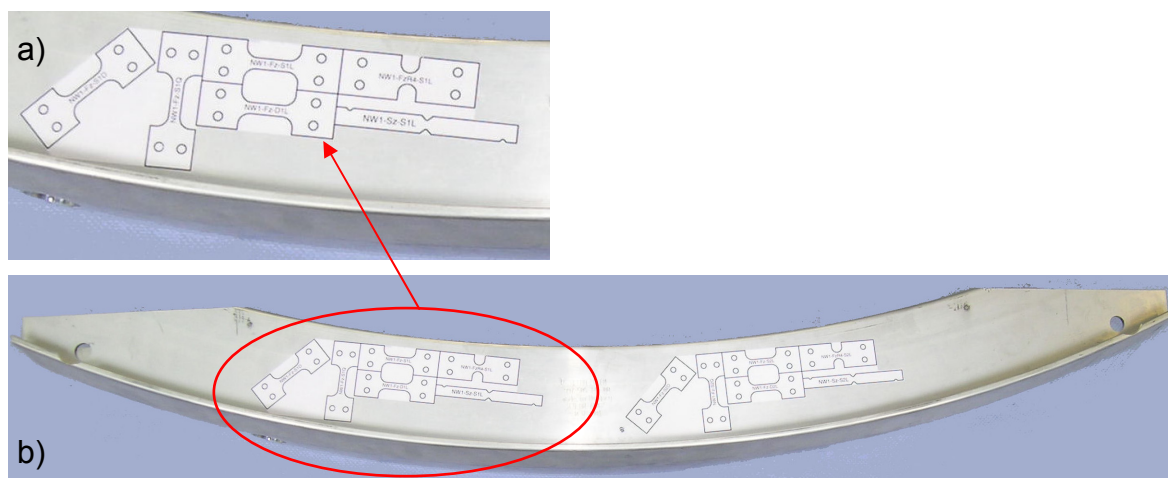


Fig. 1: a) one position of specimen extraction for material characterisation, b) geometry of the bumper

3.1 Material characterisation

To characterise the mechanical properties of the material sub-sized flat tension specimens were taken from different positions and in different orientations from one of the components (Fig. 1) and tested under static and dynamic loading. Fig. 2 shows the measured nominal stress vs. nominal strain curves. The mechanical properties show no dependence on the position of specimen extraction, whereas a slight dependence on specimen orientation (anisotropy) can be observed. The dynamic stress vs. strain curves at a strain rate of 100/s lie about 10 % higher than the corresponding static curves. The fracture strain A increases by about 10 % and the reduction of area Z by about 4 % for dynamic loading.

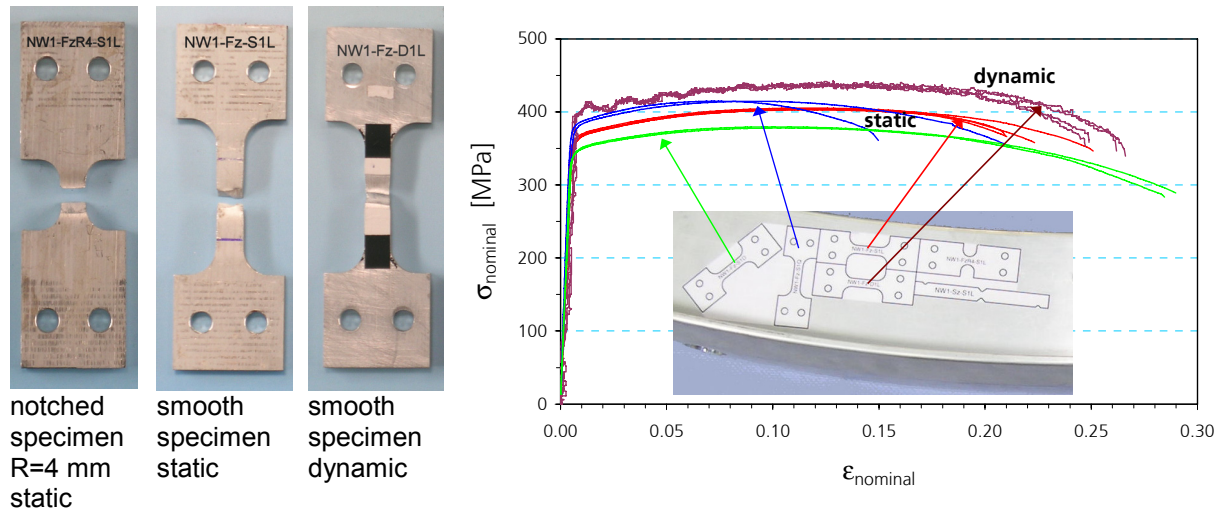


Fig. 2: smooth and notched flat tensile specimens after test and measured nominal stress vs. nominal strain curves for static and dynamic loading and for different specimen orientations (static loading)

The dependence of damage behaviour on loading type which is characterised by the stress triaxiality σ_m/σ_e was quantified by tension tests on smooth and notched specimens and shear tests.

The test set up of the modified losipescu shear test (Fig. 3) corresponds to an asymmetric four point bending and the cross section between the two notches is loaded under pure shear [8]. A detailed analysis of the fracture process of a losipescu specimen, however, gives the indication that the first damage occurs not in the pure shear region between the notches but in a tension region close to the notch root. After damage initiation the rupture of the losipescu specimen occurs through shearing. Fig. 3 shows the losipescu specimens after test, the measured nominal stress vs. displacement curves are shown in Fig. 5 together with the simulation results.

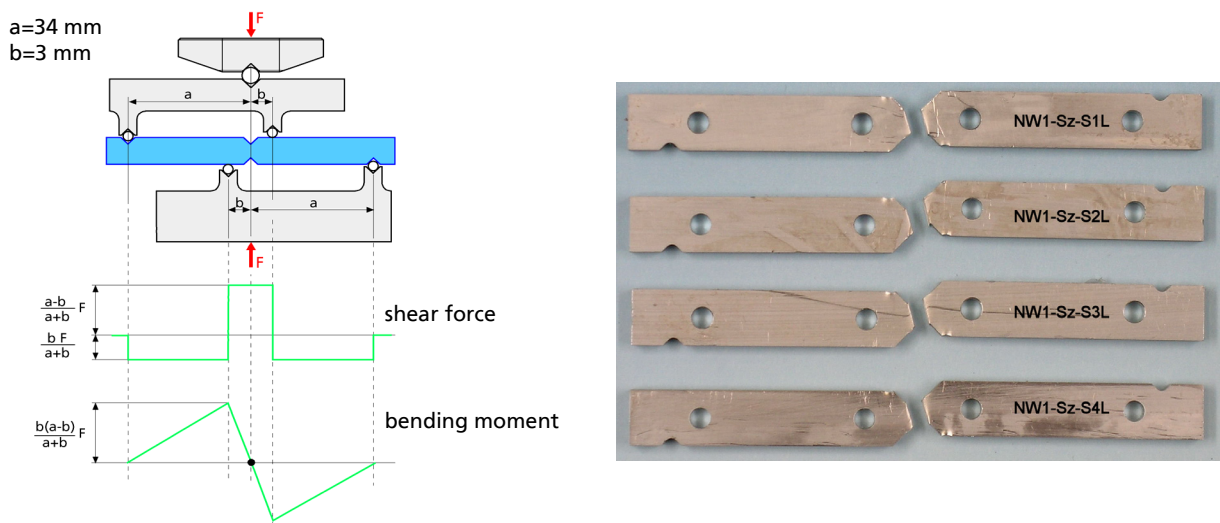


Fig. 3: schematic drawing of the modified losipescu shear test and shear specimens after test

3.2 Determination of damage parameters

All tests concerning this component were simulated with two damage models: the Gurson model and the Johnson-Cook model.

The Gurson model has seven parameters which are not independent from each other. Three of them (ϵ_n , S_n , q_1) were taken from literature [2, 7] and the remaining four parameters (f_0 , f_n , f_c and f_f) were determined by simulating the tension tests on the smooth specimens. The initial porosity f_0 and the volume fraction of void forming particles f_n were selected on the basis of results of similar materials and the corresponding critical parameters f_c (porosity at coalescence) and f_f (porosity at fracture) were determined by fitting the calculated displacement at fracture to the measured values. Fig. 4 shows that the Gurson parameters obtained from the smooth tension specimens can be used to predict the damage behaviour of the notched specimens.

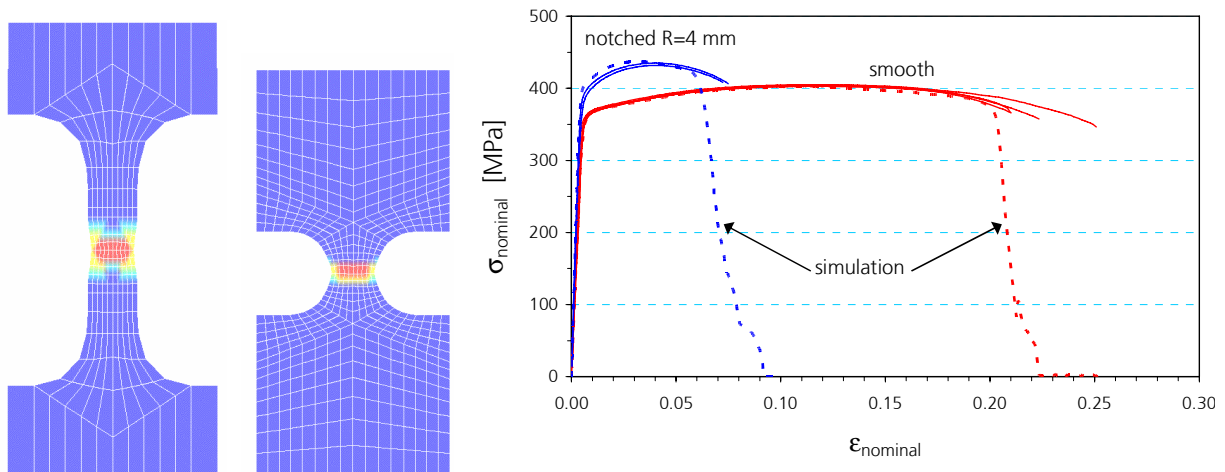


Fig. 4: contour plots of the Gurson damage variable f shortly before the onset of damage and comparison between the measured and simulated nominal stress vs. nominal strain curves for the tension tests

The finite element models used for the determination of the Gurson parameters (Fig. 4) consist of shell elements with an element length of 0.5 mm, whereas the element length in the model of the bumper is about 5 mm as used in vehicle simulations. Since the Gurson parameters are not independent of element size, they were calibrated by modelling a tension test on a smooth flat specimen with different element sizes. In this case the f_c - and f_f -values were calibrated as a function of element edge length. In the crash code LS-DYNA this relationship between the Gurson parameters f_c , f_f and element edge length can be used as input for component simulations.

For the determination of the parameters d_1 , d_2 and d_3 of the Johnson-Cook damage model the equivalent plastic strain at failure was evaluated from the experiments and simulations for different triaxialities (shear tests $\sigma_m/\sigma_e \approx 0$, smooth tension tests $\sigma_m/\sigma_e \approx 1/3$, notched tension tests $\sigma_m/\sigma_e \approx 0.5$). The parameters d_1 , d_2 and d_3 were obtained by fitting a curve of the form given in section 2.2 through these three points. The parameter d_4 was set to zero, i.e. dependence of fracture strain on strain rate was not accounted for.

The numerical results for the modified Iosipescu shear tests calculated with the Gurson and the Johnson-Cook models are shown in Fig. 5. The Johnson-Cook model can predict the shear failure using the parameters calibrated before. The Gurson model overestimates the displacements at failure of the Iosipescu specimens. This is not surprising because the void growth in the Gurson model depends only on the hydrostatic stress. Thus, shear deformation does not influence the damage process in the Gurson model which is a shortcoming of the model. As mentioned in section 2.1 the Gurson model has been extended to simulate shear failure and is available in the new version 971 of LS-DYNA. Using the extended Gurson model (Gurson/Johnson-Cook) the results of the shear tests can be predicted.

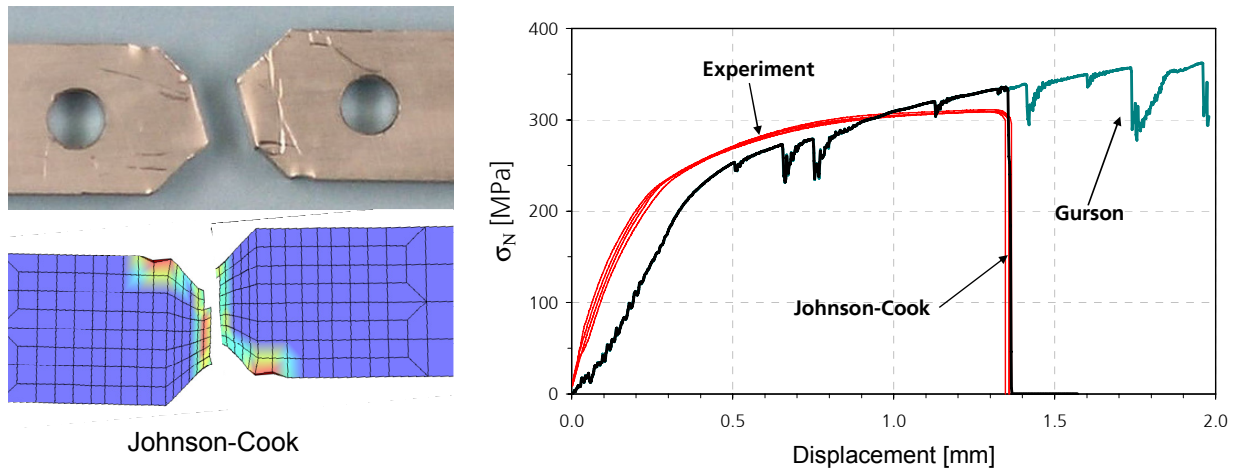


Fig. 5: comparison of fracture patterns and nominal stress vs. displacement curves between experiment and simulations for the Iosipescu shear tests

3.3 Component tests on a bumper and simulations

To verify the applicability of the two damage models (Gurson, Johnson-Cook) with the damage parameters determined before for component simulations three bumpers were tested under three-point bending. The scatter between the measured load vs. displacement curves (Fig. 6) is small. In two of the tested bumpers the development of a crack in longitudinal direction (Fig. 6) was observed which was possibly caused by an extrusion seam. The presence of this flaw in the component partly causes the slight differences between the damage patterns in experiment and simulation. The comparison of the deformation (Fig. 7) and the load vs. displacement curves (Fig. 6) shows a good agreement between experiment and simulation with the Gurson model. The agreement is equally good for the simulation with the Johnson-Cook model. The simulation without taking into account damage overestimates the load-carrying capacity of the bumpers.

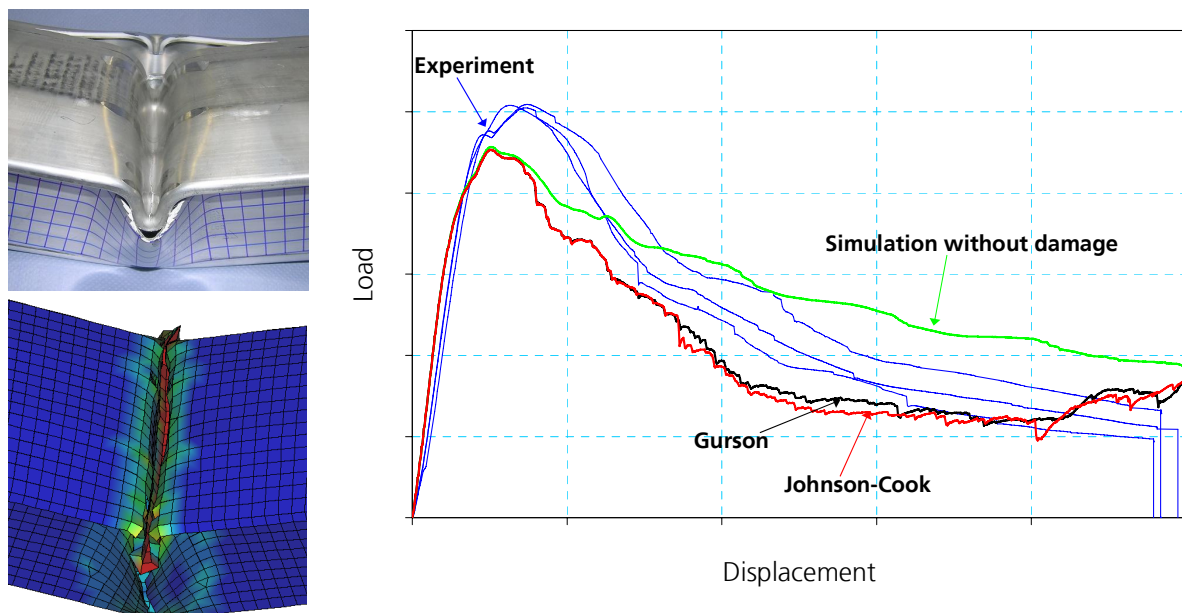


Fig. 6: damage pattern in experiment and simulation (Gurson model) and measured and calculated load vs. displacement curves for the three-point bending tests on the bumpers

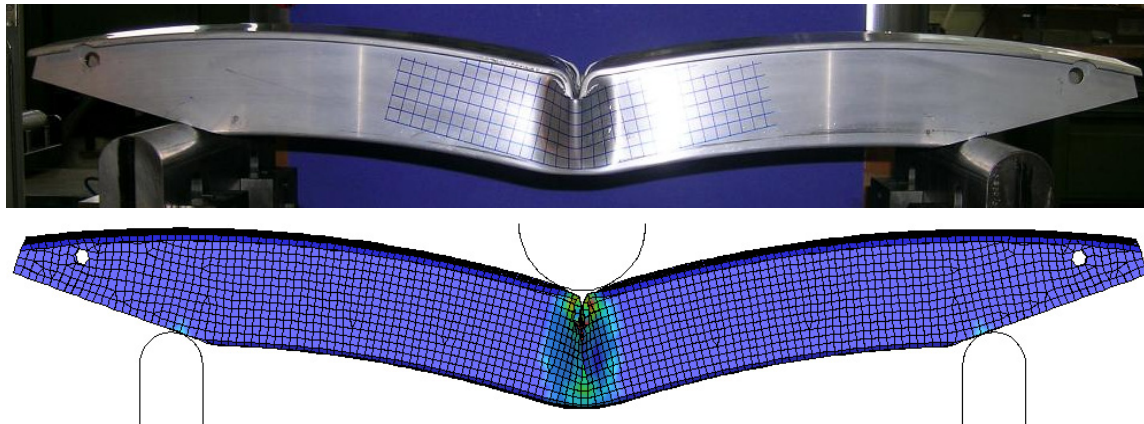


Fig. 7: bumper after three-point-bending-test and result of simulation (Gurson model)

4 Crash behaviour of an aluminium die cast alloy component

As a second example the crash behaviour of an aluminium die cast alloy component was investigated. A component and the test setup for three-point bending are depicted in Fig. 8.

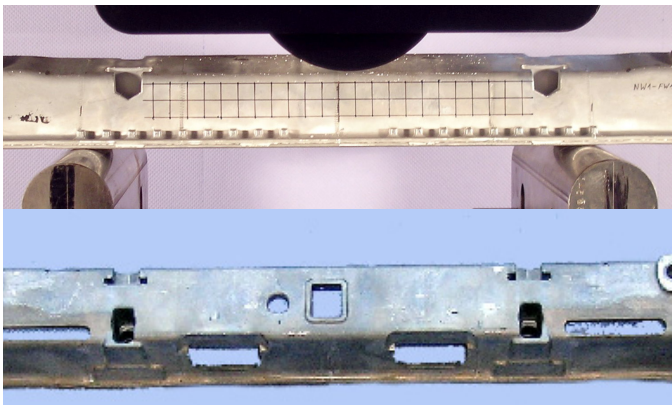


Fig. 8: geometry of a component and test setup for bending tests

4.1 Determination of material properties and damage parameters

The mechanical properties of the aluminium alloy were determined from tests on sub-size flat tension specimens under static and dynamic loading. The flow stress $R_{p0.2}$ and the ultimate tensile strength R_m at a strain rate of 100/s are about 10 % higher than for static loading, the fracture strain A and the reduction of area Z show an increase of 100 % resp. 30 % for dynamic loading.

The damage parameters of the Gurson model for the chassis material were obtained by simulation of a tension test on a smooth flat specimen and calibrated for element lengths up to 10 mm in the same way as for the first component (section 3.2). In addition to the tension tests on the smooth specimens results of tension tests on notched specimens and shear tests were available for the determination of the Johnson-Cook parameters. Fig. 9 shows the equivalent plastic strain at failure for the different triaxialities evaluated from these experiments and simulations together with the Johnson-Cook failure curve (dotted line) fitted through these points. The curve for the Gurson model in the diagram in Fig. 9 corresponds to the equivalent plastic strain for which the critical porosity f_c is reached using the Gurson parameters determined before. For triaxiality values between 0.2 and 0.6 the two curves are in the same range, whereas the curves differ for triaxialities below 0.2 and above 0.6. For low triaxialities the Gurson curve approaches infinity, which is the reason why the Gurson model cannot predict shear failure. For the phenomenological Johnson-Cook model the failure strain under shear loading could be determined from the shear tests. For triaxialities above 0.6 no test results were available and the run of the Johnson-Cook failure curve in this region is an extrapolation and given by the choice of the parameters d_1 , d_2 and d_3 to best fit the available data.

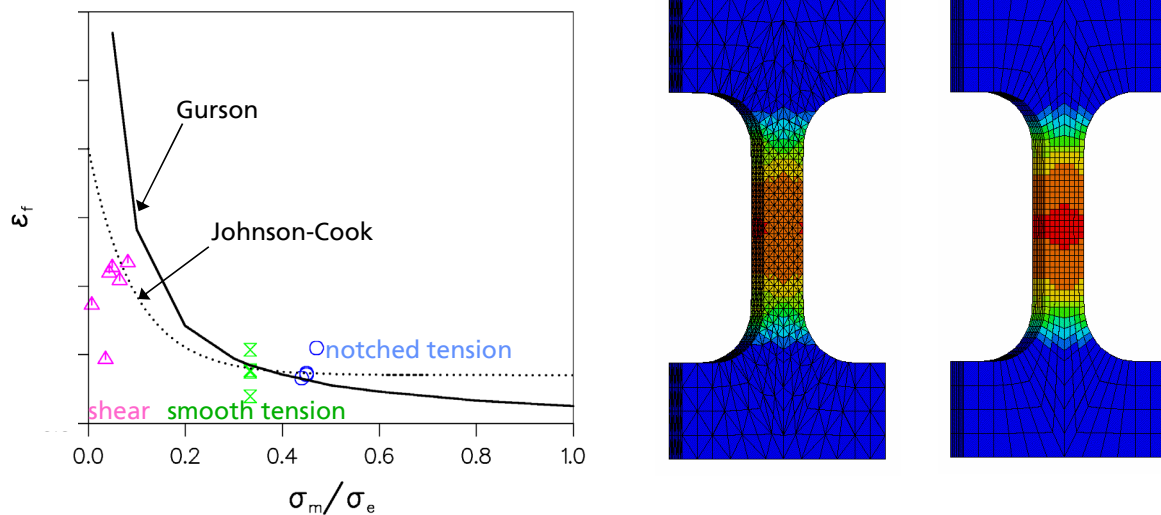


Fig. 9: plastic failure strain vs. stress triaxiality for the Gurson and Johnson-Cook models and contour plots of the Johnson-Cook damage variable D shortly before the onset of damage for smooth tensile specimens modelled with TET4 and HEX8 elements

The finite element model of the cast alloy component was composed of four-noded tetrahedron (TET4) elements with an edge length of about 5 mm. For this reason the transferability of the parameters of the two damage models between different element types was investigated. The tension tests were simulated with shell elements, TET4 elements and HEX8 elements (eight-noded hexahedra). Contour plots of the Johnson-Cook damage variable D shortly before the onset of fracture for the TET4 and HEX8 meshes are shown in Fig. 9. It was found that in this case for both the Gurson and Johnson-Cook model the same set of damage parameters can be used for the three element types.

4.2 Bending tests and simulations

As a load case example three components were tested under three-point bending (Fig. 8). The development of damage (Fig. 12a) was similar for all three tested components although the crack initiation and propagation occurred at different punch displacements, which can be recognised from the measured load vs. displacement curves in Fig. 11.

Two different finite element models with TET4 elements were used for the simulations of the bending tests. Unlike the component geometry (Fig. 10a) the centre section of the first model (Fig. 10b) was generated symmetrically with holes on both sides, while the second model (Fig. 10c) corresponds to the component geometry which is unsymmetric with a hole on one side and an additional rib on the other. By this asymmetry the location of damage is predetermined in the component and was also predicted by the unsymmetric model, whereas in the simulation with the symmetric model damage can occur on both sides and did occur on the wrong side.

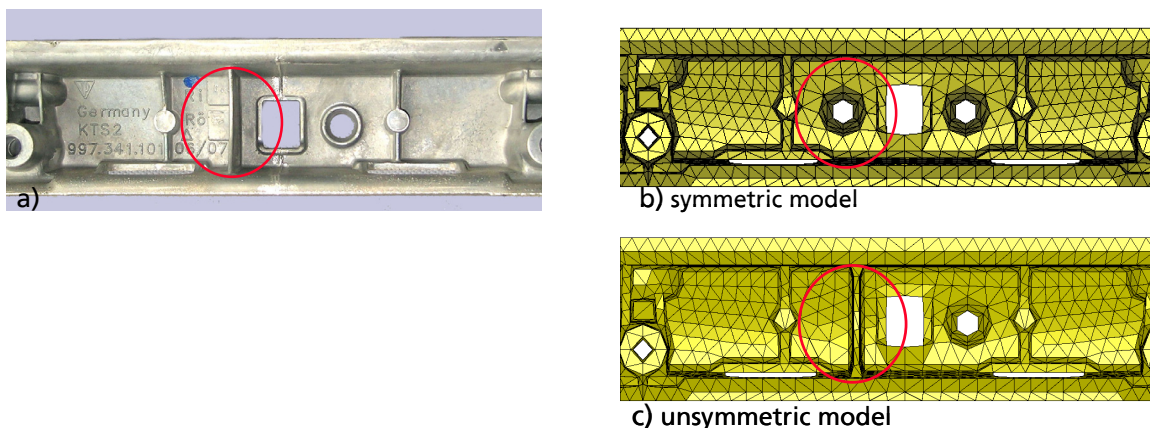


Fig. 10: a) component geometry of the centre section, b) and c) geometries of two different finite element models

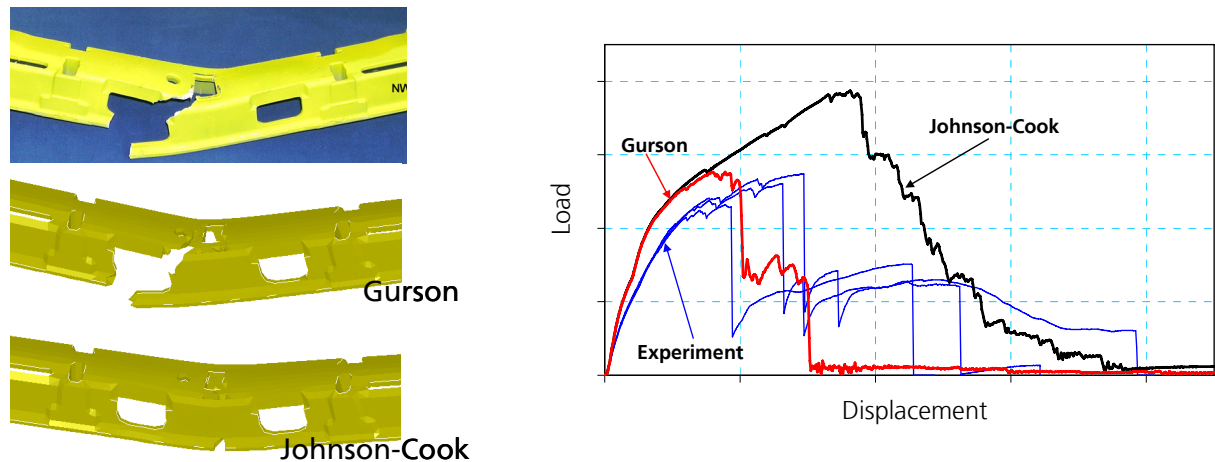


Fig. 11: damage pattern in experiment and simulations and measured and calculated load vs. displacement curves for the bending tests

The bending tests were simulated with the Gurson and the Johnson-Cook model using the damage parameters determined for the material. For this load case, however, different fracture patterns were calculated with the two damage models (Fig. 11). The simulation with the Johnson-Cook model predicted cracking in the middle of the component section, whereas the fracture pattern calculated with the Gurson model is in very good agreement with the experiments. Fig. 12b shows the different positions of maximum damage calculated with both models.

An evaluation of the stress triaxiality at the location of initial damage in experiment and simulation with the Gurson model yielded a very high value of 1.5. For such high triaxiality values no tests on laboratory specimens were available for the determination of the fracture strain for the Johnson-Cook model. The Johnson-Cook parameters obtained from tension and shear tests (Fig. 9) underestimate the development of damage at high triaxialities, whereas the Gurson parameters are also applicable at high triaxialities without further experiments. A simulation with the Johnson-Cook model and a failure curve which was fitted to the failure strain of the Gurson model at high triaxialities lead to consistent results.

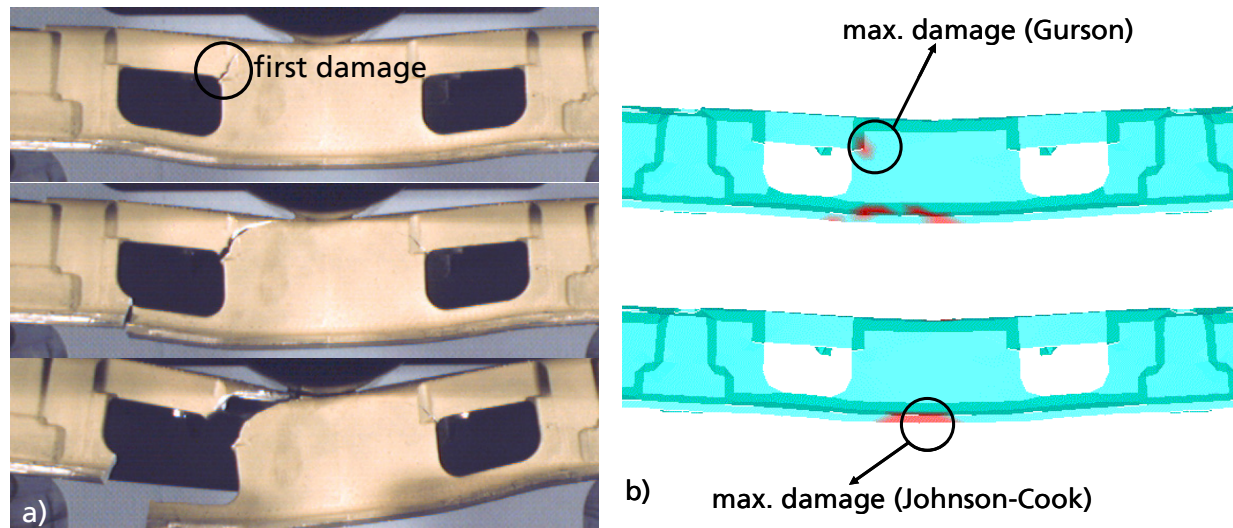


Fig. 12: a) development of damage during the bending test, b) distribution of the damage variables f (Gurson model) and D (Johnson-Cook model) before the onset of failure

In the simulations of the bending tests described above the LS-DYNA element formulation (ELFORM) 10 was used for the four-noded tetrahedron elements of the component mesh. As can be seen from the load vs. displacement curves in Fig. 11 the response calculated with this element formulation with one point integration is too stiff. Additional simulations were performed using ELFORM 13 (one point nodal pressure tetrahedron for bulk forming) and ELFORM 16 (five point ten-noded tetrahedron). The load vs. displacement curves calculated with the different element formulations for the Gurson and

Johnson-Cook model are shown in comparison with the experimental results in Fig. 13. No difference can be observed between the results obtained with ELFORM 10 and 13 for this load case. For ELFORM 16 the stiffness of the model before the onset of damage is very much reduced and the agreement between experiment and simulations concerning the development of damage and the load-carrying capacity after initial damage has been improved. For the simulation with the Johnson-Cook model and ELFORM 16 the calculated damage pattern (Fig. 13) now matches the experimental one without a change of parameters. It has to be mentioned, however, that for the improvements achieved by using ELFORM 16 the computational cost of a simulation increases by a factor of ten.

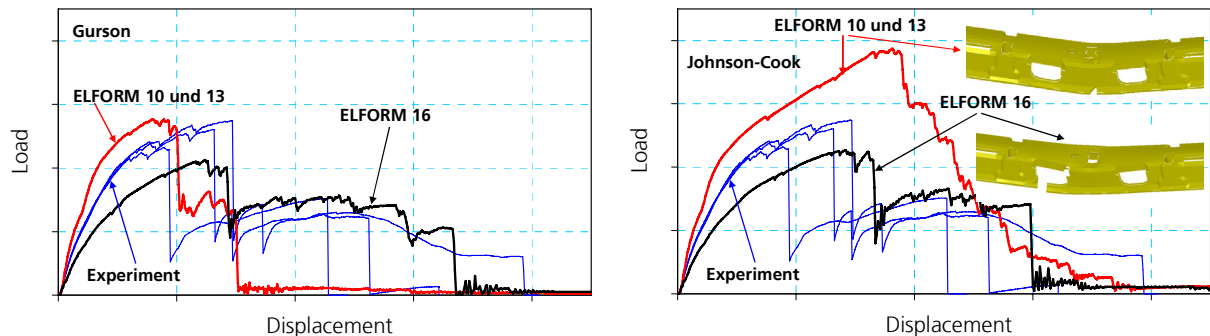


Fig. 13: load vs. displacement curves calculated with different element formulations for the Gurson model (left) and Johnson-Cook model (right) in comparison with the experimental results and damage pattern calculated with the Johnson-Cook model and ELFORM 16 (right)

5 Conclusions

Relevant characterisation and reliable modelling of deformation and damage behaviour are necessary for the assessment of crash safety of load-bearing automobile components especially of new light weight alloys. For this purpose an evaluation chain including material characterisation, numerical simulation with a suitable damage model, determination of damage parameters for the chosen damage model and verification by component tests has been established and was applied to two automobile components. An extruded aluminium profile and a component from an aluminium die cast alloy were characterised under crash relevant loading and simulated with the micromechanical Gurson model and the phenomenological Johnson-Cook damage model.

The influences of the stress triaxiality and strain rate on the deformation and damage behaviour were taken into account in the experimental and numerical investigations. The damage parameters of the Gurson model can be obtained by simulation of tension tests only, whereas experiments at different triaxialities are required for the determination of the failure strain for the phenomenological Johnson-Cook model. The failure strain for the Johnson-Cook model was determined from tension tests on smooth and notched specimens and shear tests, but it was found that additional tests at high triaxialities (fracture mechanics tests) would be needed for a reliable prediction of damage behaviour. Disadvantages of the Gurson model are that its parameters are dependent on element size and have to be calibrated and that it cannot predict shear failure. This second difficulty was overcome by using the Johnson-Cook failure criterion in the region between pure shear and uniaxial tension in an extended version of the Gurson model which has been implemented in LS-DYNA. The formulation of the tetrahedron elements affects the numerical results concerning the stiffness and damage behaviour. The applicability of the two damage models for crash simulation was demonstrated by simulation of the component tests in different crash relevant load cases.

6 Literature

- [1] Sun, D.-Z., Feucht, M., Frank, T., Andrieux, F., Böhme, W., Charakterisierung und Modellierung des Versagensverhaltens von Strukturkomponenten aus hochfesten Stählen für die Crashsimulation, crashMAT2004, 27.-28.04.2004, Feiburg
- [2] Needleman, A. and Tvergaard, V., Analysis of Ductile Rupture in Notched Bars, J. Mech. Phys. Solids 32 (1984) 461-490.
- [3] Gologanu, M., Leblond, J.B., Perrin, G., Devaux, J., Recent Extensions of Gurson's Model for Porous Ductile Metals, Continuum Micromechanics, CISM Courses and Lectures No. 377, ed. by P. Suquet (1997) 61-130.

- [4] Wilkins, M.L., Streit, R.D., Reaugh, J.E., Cumulative-strain-damage model of ductile fracture: simulation and prediction of engineering fracture tests, UCRL-53058 Distribution Category UC-25, Lawrence Livermore Laboratory, University of California, Livermore 1980.
- [5] Johnson, G.R., Cook, W.H., Fracture characteristics of three metals subjected to various strains, strain rates, temperatures and pressures, Engineering Fracture Mechanics, vol.21, No.1, pp.31-48, 1985.
- [6] Andrieux, F., Sun, D.-Z., Riedel, H., Development and application of a micromechanical model for the description of the growth and coalescence of spheroidal voids, IFAMST 4th International Forum on Advanced Science and Technology, July 4 to 7, 2004 in Troyes, France
- [7] Sun, D.-Z., Hömig, A., Böhme, W., Schmitt, W., Application of micromechanical models to the analysis of ductile fracture under dynamic loading, in: Fracture Mechanics 25th Volume, ASTM STP 1220, ed. by F. Erdogan, American Society for Testing and Materials, Philadelphia, 1995, 343-357.
- [8] Xing, Y.M., Poon, C.Y., Ruiz, C., A whole-field strain analysis of the Iosipescu specimen and evaluation of experimental errors, Composites Science and Technology 47 (1993), 251-259

